World Academy of Science, Engineering and Technology
International Journal of Mechanical and Mechatronics Engineering
Vol:11, No:2, 2017

Feasibility Study of the Quadcopter Propeller Vibrations for the Energy Production

Nneka Osuchukwu, Leonid Shpanin

***Abstract*—**The concept of converting the kinetic energy of quadcopter propellers into electrical energy is considered in this contribution following the feasibility study of the propeller vibrations, theoretical energy conversion, and simulation techniques. Analysis of the propeller vibration performance is presented via graphical representation of calculated and simulated parameters, in order to demonstrate the possibility of recovering the harvested energy from the propeller vibrations of the quadcopter while the quadcopter is in operation. Consideration of using piezoelectric materials in such concept, converting the mechanical energy of the propeller into the electrical energy, is given. Photographic evidence of the propeller in operation is presented and discussed together with experimental results to validate the theoretical concept.

***Keywords*—**Unmanned aerial vehicle**,** energy harvesting, piezoelectric material, propeller vibration.

I. Introduction

THE quadcopter presents a lot of promise for a variety of applications, such as the aerial imaging for media, mapping or real estate purposes, etc. However, they are held back due to their high power demands which cause short operational time. Thus, one of the major limitations of quadcopters is their short battery life. It is challenging to improve this as the use of a larger battery will increase both the load and the power usage of the quadcopter. From the previous works, different energy harvesting techniques have already been investigated for the quadcopter operation, where the energy recovery was produced from Photovoltaic Cells (solar) and Thermoelectric Generators (heat) [1]-[3]. Consideration of using the piezoelectric energy harvester for rotary motion and other applications were investigated previously [4]-[6] demonstrating that using the piezoelectric materials is possible in the piezoelectric energy harvester structures for low rotary motion applications [4]. In contrast, the present work investigates a fundamental new approach of extracting the kinetic energy from the propellers of the quadcopter, once they are rotating, with further consideration of using the piezoelectric energy harvester which could potentially convert the kinetic energy into electrical energy and to use this energy for the quadcopter operation.

This contribution researched how a new form of the energy harvesting mechanism could potentially provide a solution for extending the flight time of the quadcopter via extra energy production. A novel technique of energy production for the quadcopter operation is described proposing a method which is based on the quadcopter propeller vibrations and aims to increase the operational time of quadcopter while the propellers are rotating. The attempt to model the energy production of such mechanism theoretically, while examining the quadcopter propeller at different test conditions, is presented using the SolidWorks 3D CAD software.

N. Osuchukwu and L. Shpanin are with the Faculty of Computing, Engineering and Environment, School of Mechanical, Aerospace and Automotive Engineering, Coventry University, Coventry CV1 2JH, UK (e-mail: osuchukn@coventry.ac.uk, leon.shpanin@coventry.ac.uk).

II. Development of the Quadcopter Energy Harvester

A piezoelectric energy harvester study carried out by previous authors [4], [6] showed that the rotary motion applications are capable of producing vibrations of the piezoelectric energy harvester that can further convert this kinetic energy to the electrical energy. However, in the previous study, a tip mass was mounted on the piezoelectric energy harvester for the production of harvester oscillations during the rotation of the rotary motion devices [4], [6]. A major drawback of increasing the mass of piezoelectric material in the quadcopter is the introduction of weight to the system, as this additional mass can affect the aerodynamic performance of the vehicle. In an attempt to circumvent this issue, an investigation into the use the quadcopter propeller in conjunction with the piezoelectric energy harvester that does not require a tip mass for the piezoelectric harvester vibrations is proposed in this paper.

A. Conceptual Design

The conceptual design of using four quadcopter propellers having two piezoelectric energy harvesters mounted on the top and another two at the bottom parts of each propeller is shown in Fig. 1. The placement of the piezoelectric energy harvesters would alter the volume of energy harvested by the system. Therefore, it was necessary to simulate a single propeller's energy scavenging capabilities, to carry out an investigation in order to determine the ideal placement of a single piezoelectric energy harvester mounted on the propeller in order to then, in the future, scale this value to obtain an estimate for the entire system of eight (top/bottom) piezoelectric energy harvester components.

B. Propeller Model Conditions

As the creation of a CAD propeller model was not a fundamental part of this investigation, whereas the evaluation of the propeller itself was the focus, the use of a premade model similar to Gemfan 1147 ABS propeller was used [8]. The propeller model used for this evaluation was obtained from the online community GrabCAD. GrabCAD offers designers and engineers a free library to which they can download and upload publicly accessible CAD models that

can be altered. As the largest source of mechanical engineering content, it is used by engineers to increase the speed of the design process [8]. Fig. 2 shows the investigated propeller. The propeller model used in CAD simulations (Fig. 2 (a)) was created by a Certified SolidWorks Expert (CWSE) [9]. As this model had been obtained from an open source, it was compared against an actual Gemfan 1147 propeller [7], shown in Fig. 2 (b), to ensure it was a true representation.

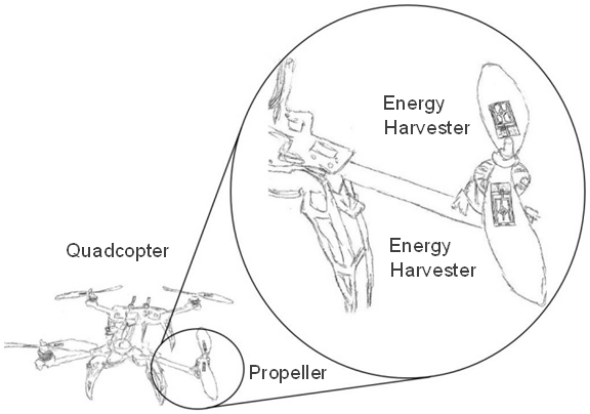

Fig. 1 Conceptual design of piezoelectric energy harvesting system applied to a quadcopter with Gemfan 1147 ABS propeller [7]

(a) (b)

Fig. 2 Gemfan 1147 propeller shape identification: (a) CAD Model of Gemfan 1147, (b) Actual Gemfan 1147 propeller

The rotational symmetry of the propeller design allowed for certain measurements to be taken on a single side and assumed for the other. The measurements taken were of key design parameters. Fig. 3 shows the locations, labelled A-E of the Gemfan 1147 propeller CAD model. These locations were used for both the CAD model and actual propeller during theoretical and experimental result evaluations. Table I shows a comparison of the CAD and actual Gemfan 1147 propellers, with the dimensions following the same numbering system shown in Fig. 3. These measurements were taken using the inbuilt 'measure' tool provided by SolidWorks CAD software. Table II shows the ABS plastic properties used in propeller CAD model which are similar to the Gemfan 1147 propeller [7]. Despite this, the propeller CAD model tolerance of +3% is considered as a largest error and is a reasonable representation of the actual propeller.

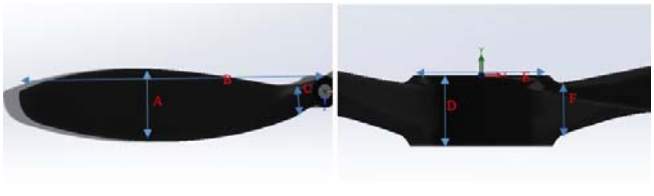

(a) (b)

Fig. 3 Diagram of the Gemfan 1147 CAD model with annotated dimension locations shown in Table I, (a) View from top, (b) View from front

TABLE I
CAD MODEL AND ACTUAL GEMFAN 1147 PROPELLER COMPARISON

Dimension	CAD Model	Actual Propeller	Percentage Error, %
		Length, mm	
A	29.99	30.55	1.83
B	137.97	139.68	1.22
C	11.41	11.54	1.13
D	6.83	6.75	-1.19
E	13.2	13.28	0.602
F	4.93	5.01	1.60
		Mass, kg	
	0.0097	0.01	3

TABLE II
MATERIAL PROPERTIES OF ABS PLASTIC USED IN CAD MODEL PROPELLER

Property	Value	Units
Elastic Modulus	2000000000	N/m^2
Poisson's Ratio	0.394	N/A
Shear Modulus	318900000	N/m^2
Mass Density	1020	kg/m^3
Tensile Strength	30000000	N/m^2
Thermal Conductivity	0.2256	W/(m.K)
Specific Heat	1386	J/(kg.K)

C. Propeller Simulation Setup and Test Parameters

For the simulated tests, using SolidWorks, it was important to ensure that the setup used was as close to the operational environment of the propeller as possible. During the Linear Static and Frequency analyses, the two main features to consider for this were the definition of fixtures and loads. Fixtures were used to describe the way how the model was supported by the motor mounts, with loads being used to introduce the simulated effect of the turning motor which was excluded from the analysis. Fig. 4 shows the fixtures used for simulations. The blue arrows indicate faces of the model that are restricted using the 'Fixed Hinge' fixture, this type of restraint results in the selected circular faces only being able to rotate around their own axis, chosen to represent the interaction between the propeller and the motor mount. In this same figure the green arrows show the planar faces that were restrained using the 'Roller/Slider' fixture. This fixture type limited the selected faces to moving freely within their own plane, without allowing it to move in a direction that was normal to their plane. Once the fixtures had been applied, the external load type was then selected. To replicate the turning force applied by the quadcopter motor, the centrifugal load type was selected. This allowed for an angular velocity to be

applied to a selected reference for direction. In this case, the selected reference was an axis created in the centre of the propeller hub; the centrifugal load direction is shown by the red arrow in Fig. 4. As the model used was a Counter Clockwise (CCW) propeller the direction was chosen in keeping with this. Fig. 4 shows an actual propeller with mount attachment to highlight the points of interaction between the propeller and the mount, and its orientation in the selected volume of air around it using the inbuilt SolidWorks Wizard shown in Fig. 5.

Fig. 4 An example of simulated Gemfan 1147 propeller fixtures

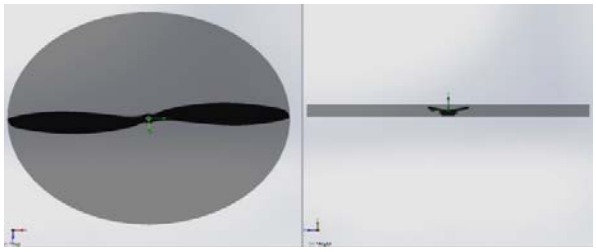

(a) (b)

Fig. 5 An example of model propeller position in SolidWorks flow simulation study. (a) Top view propeller, (b) Front view propeller

The simulation tests carried out in this contribution were the linear static simulation from 1000 to 8000 revolution per minute (rpm) of the propeller. These were used to provide an indication of the points of maximum deflection on the propeller which was further compared to the experimental results where the actual Gemfan 1147 propeller was tested under similar rpm propeller conditions. To validate the modeling work, the CAD model propeller thrust was simulated and experimentally validated under similar test conditions. The visual data acquisition tool used was a "Photron FASTCAM Mini UX100" high-speed camera. This camera was set to a resolution of 1280 x 400 pixels, capturing 5582 frames at a frame rate of 12500 frames per second (fps). During testing the propeller, rpm was a controlled factor, with the resulting thrust, voltage, and current of a Turnigy Multistar 3525-850 kV 14Pole Multi-Rotor Outrunner set up for CCW rotation recorded. Evaluation of propeller deflection was carried out later during evaluation of the high-speed camera footage through slow motion analysis.

III. Experimental Results

Fig. 6 shows the propeller's simulated and experimental thrust results at various propeller rotational speeds. These results are presented in the numerical (Fig. 6 (a)) and graphical (Fig. 6 (b)) representation in order to validate the accuracy of the propeller modeling test conditions, and indicate the proportional relationship between simulated and experimental propeller rotational speed and the thrust generated.

Table III shows the result comparison of the experimental and simulated propeller frequency of rotations. The maximum simulated error value was approximately 3.28%, considered to be adequate representation of the propeller behavior.

Speed (RPM)	Experimental Thrust (N)	Simulated Thrust (N)
1081	0.254972901	0.245059
2006	0.872791853	0.881032
3002	1.873070155	1.95379
4007	3.39310091	3.35924
5016	5.374044216	5.45503
6003	7.629573722	8.22966
7007	10.76770173	11.8125
7983	13.93524969	15.1706

(a)

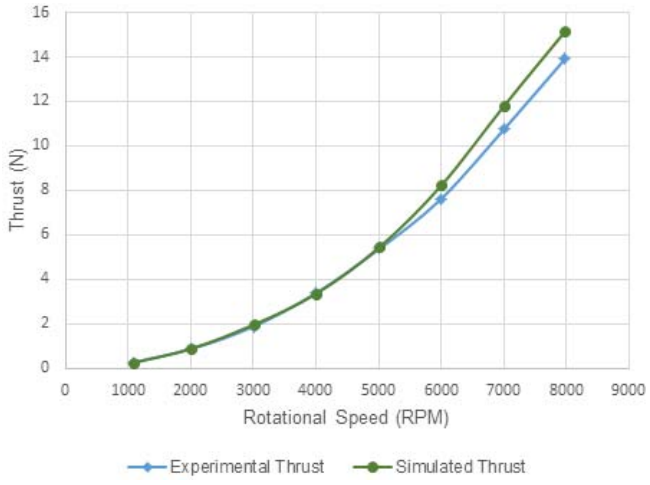

(b)

Fig. 6 Comparison of experimental and simulated propeller thrust results. (a) Numerical results representation, (b) Graphical representation of the results

From the simulated animation results the propeller deflection was observed from 1081 rpm to 7983 rpm. A typical example is shown in Fig. 7 where the propeller deflection changed from 1.9 mm (Fig. 7 (a)) to 3.6 mm (Fig. 7 (b)).

The same trend, shown in Fig. 7, is observed in the experimental results using the high-speed camera results. At a constant speed of 7983 rpm, the propeller tip had deflected from its previously recorded location at the constant speed of

1081 rpm. From the images in Fig. 8, it was calculated that there was a change in propeller tip position of approximately 1.0 mm. The green indicator in this image indicated the stationary 40 mm position on the attached rule. The red marker was used to track the changing propeller tip position.

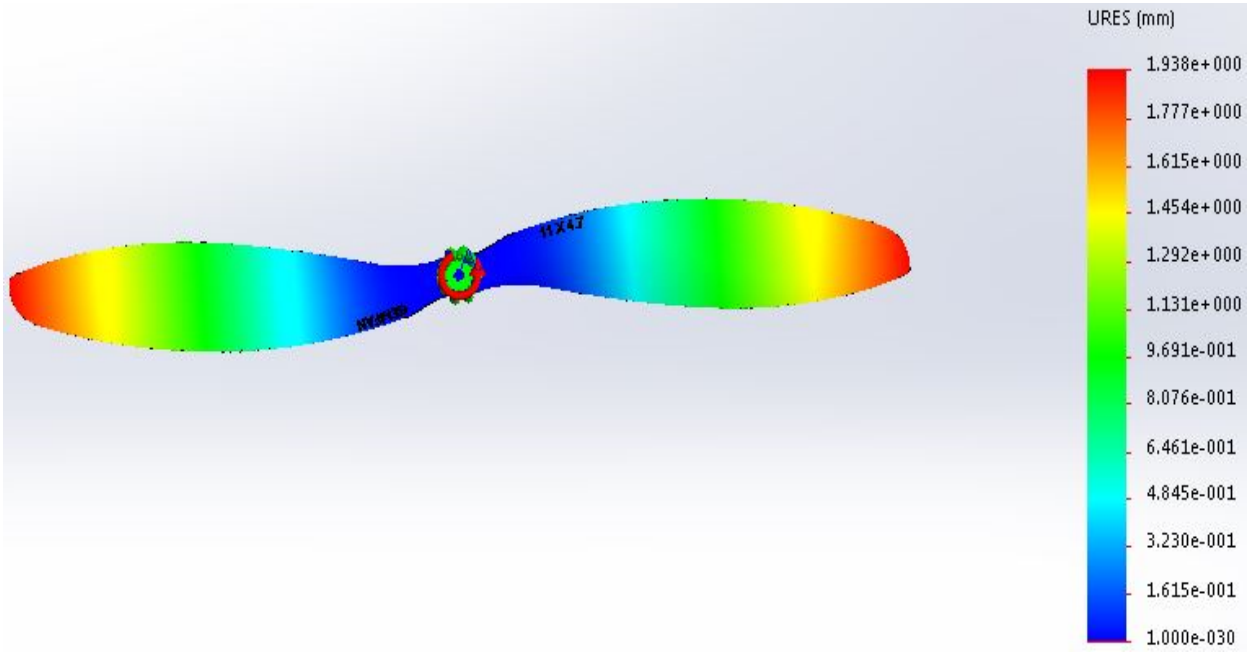

(a)

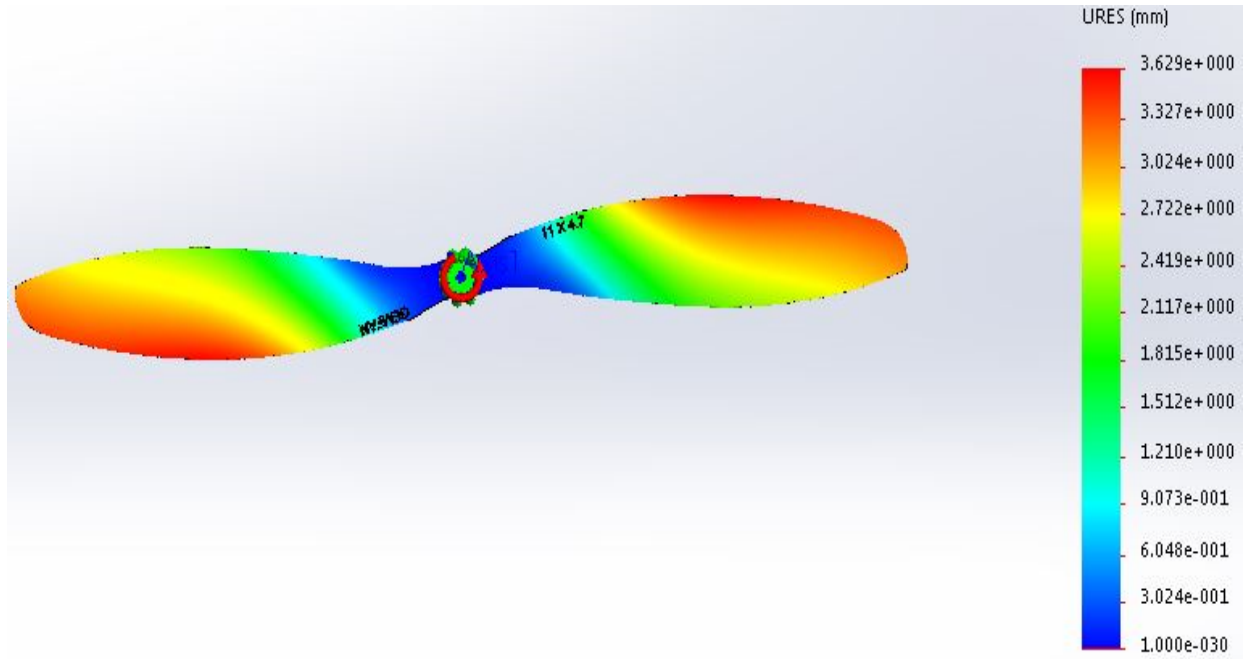

(b)

Speed (RPM)	1081	2006	3002	4007	5016	6003	7007	7983
Deflection (mm)	1.897	2.742	2.906	2.915	2.916	3.099	3.311	3.513

(c)

Fig. 7 Simulated propeller deflection results. (a) Propeller deflection at 1081 rpm, (b) Propeller deflection at 7983 rpm, (c) Maximum resultant propeller deflection at different propeller rotational speeds

TABLE III
COMPARISON OF EXPERIMENTAL AND SIMULATED PROPELLER ROTATION FREQUENCY RESULTS

Speed (RPM)	Experimental Freq. of Rotations per second (Hz)	Simulated Freq. of Rotations (Hz)	Simulated Percentage Error (%)
1081	18.01666667	17.624	2.17946346
2006	33.43333333	32.652	2.336989033
3002	50.03333333	48.797	2.47101932
4007	66.78333333	65.053	2.59096581
5016	83.6	81.313	2.735645933
6003	100.05	97.163	2.885557221
7007	116.7833333	113.2	3.068360211
7983	133.05	128.68	3.284479519

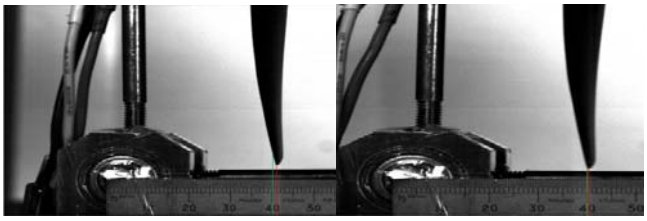

(a) (b)

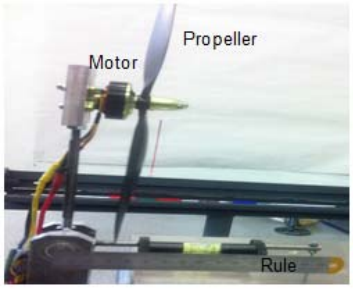

(c)

Fig. 8 Propeller deflection observed between (a) 1081 rpm and (b) 7983 rpm propeller rotations, (c) Quadcopter propeller test rig

From the SolidWorks simulated propeller deflection results, shown in Fig. 7 (c), the change in propeller deflection between two propeller rotational speeds of 1081 rpm and 7983 rpm is 1.6 mm which is in reasonable agreement with the experimental results shown in Fig. 8.

IV. DISCUSSION OF RESULTS

The results presented in section III demonstrate the possibility to model and observe the quadcopter's propeller deflection at different propeller rotational speeds, from 1081 rpm to 7983 rpm (Figs. 7 (a)-(c), and Figs. 8 (a), (b)).

From Table III and Fig. 6, the simulated propeller rotational speeds and their corresponding propeller thrust were in good agreement with the experimental results and the high-speed camera photography results (Figs. 6 and 8).

The potential position of each piezoelectric energy harvester on the propellers shown in Fig. 1 is estimated from Fig. 9. Their positions are close to the area of maximum propeller tensile stress produced by the maximum propeller deflection.

From the SolidWorks simulated results and further experimental results evaluations, it was observed that the quadcopter CCW propeller can be deflected without a tip mass at different propeller rotational speeds. The advantage of this effect may be considered for the energy generation produced by applying the piezoelectric material to the propeller where no need for a tip mass will be a main advantage, as vibrations and deflections are naturally present during operation. Such conditions allow the piezoelectric energy harvester to operate at low frequencies close to the frequency range of the propeller rotation shown in Table III and less effect on the aerodynamic characteristics of the quadcopter.

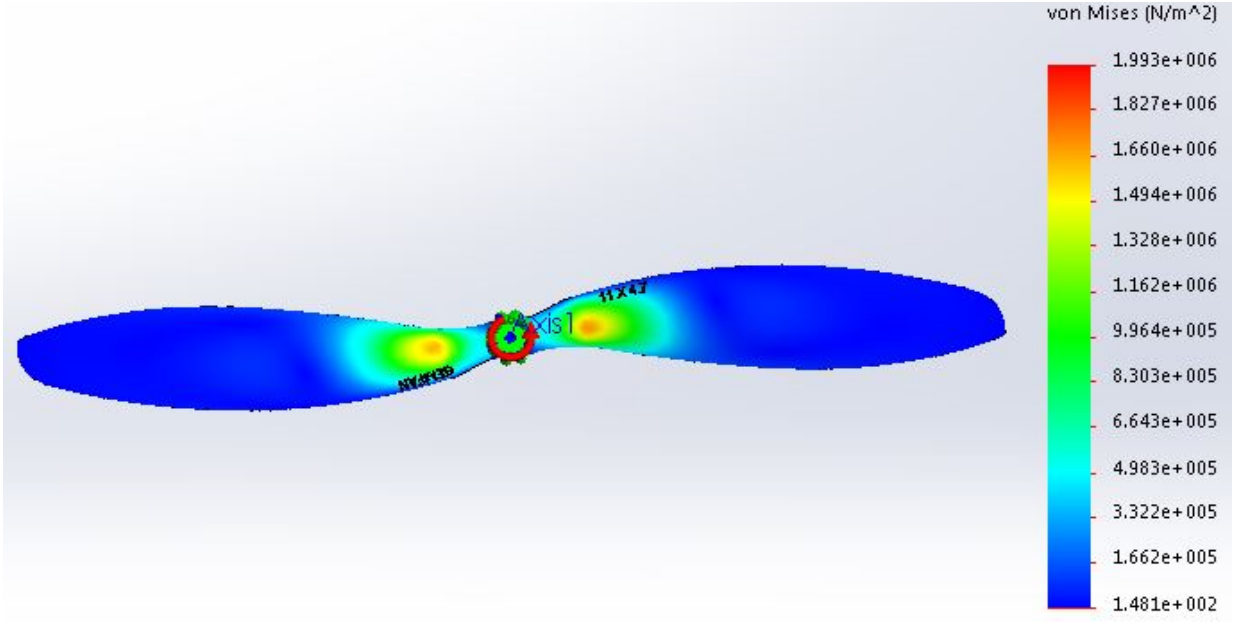

(a)

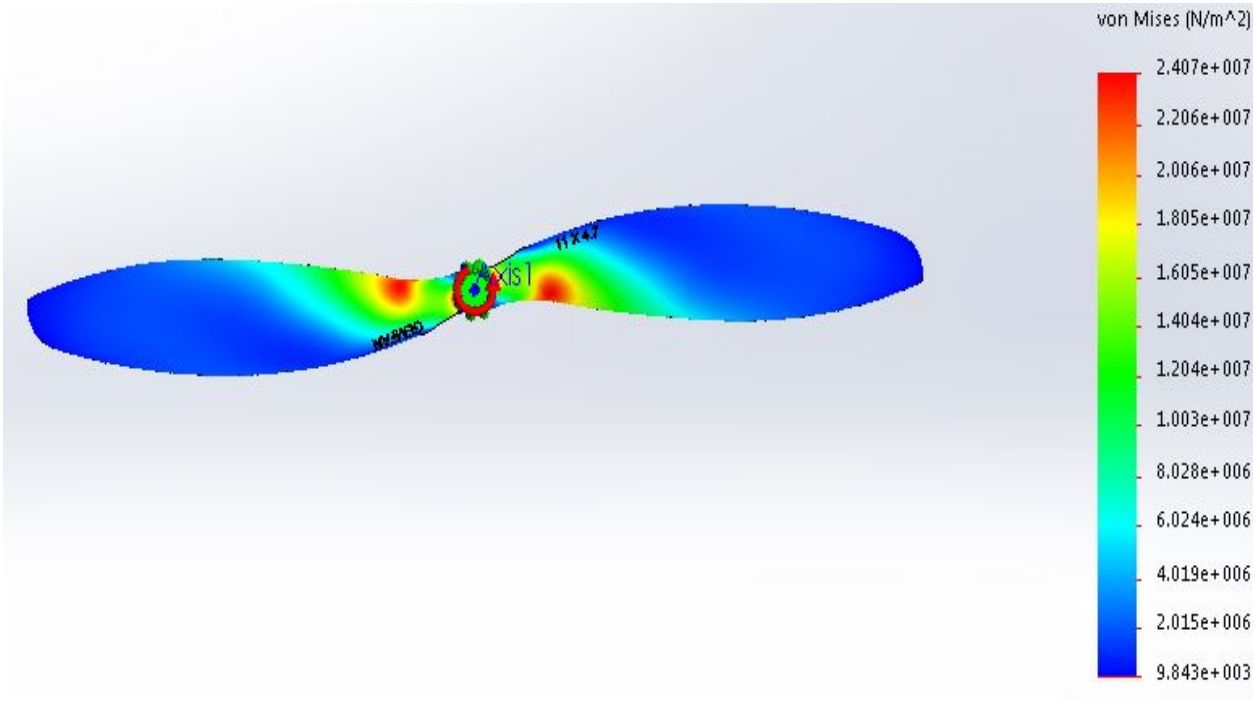

(b)

Fig. 9 An example of simulated CAD model propeller tensile strength at (a) 1081 rpm, 1.99 x 10^6 N/m^2 and (b) 7983 rpm, 2.41 x10^7 N/m^2, rotational propeller speeds

Fig. 9 suggests that the maximum propeller tensile strength is present, once the propeller rotational speed is 7983 rpm, close to the propeller fixture.

In addition, Fig. 7 (c) shows that the propeller deflection increases or decreases from the propeller rotational speed of 4007 rpm for approximately 0.6 - 1.0 mm at lower and higher propeller rotational speeds, respectively. Therefore, a dynamic flight of the quadcopter could increase the propeller deflections needed for the piezoelectric material to be vibrated.

A general concept of converting kinetic energy of the quadcopter propeller into electrical energy by applying the piezoelectric material to the propeller is shown in Fig. 10.

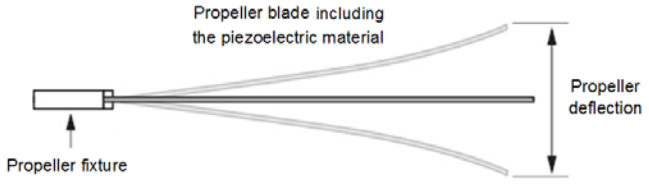

Fig. 10 A general concept of the quadcopter propeller energy production during the propeller rotation

V. Conclusion

The feasibility study of the quadcopter propeller at different constant propeller rotational speeds was investigated in this paper. In order to gain more understanding of the quadcopter propeller energy production concept, further research is required in evaluation into the behaviour of the propeller whist accelerating. Although the SolidWorks simulation results reasonably predict the quadcopter propeller behavior, further work, manufacturing of an energy harvester propeller by applying the piezoelectric materials to each quadcopter propeller (Fig. 1), as well as experimental validation of the proposed concept for the investigated propeller operating conditions is needed.

Acknowledgment

The authors appreciate the support provided by the management of the School of Mechanical, Aerospace and Automotive Engineering, Coventry University, UK that has funded this work as well as the laboratory technician, Mr. Luke Stirrup, for his assistance in conducting the experimental work.

References

[1] S. Cass, "Beyond the Quadcopter: New Designs for Drones Showcased at CeBIT", *IEEE Spectr*. 53 (5), pp.21-22, 2016.

[2] M. Shaheed, A. Abidali, J. Ahmed, S. Ahmed, I. Burba, P. Fani, G. Kwofie, K. Wojewoda and A. Munjiza " Flying by the Sun only: The Solarcopter prototype" *Aerospace Science and Technology*, vol. 45, pp.209-214, 2015.

[3] J. Fleming, W. Ng and S. Ghamaty, "Thermoelectric-Based Power System for Unmanned-Air-Vehicle/ Microair-Vehicle Applications", *Journal of Aircraft*, 41(3), pp.674-676, 2004.

[4] F. Khameneifar, S. Arzanpour, and M. Moallem, "A piezoelectric energy harvester for rotary motion applications: Design and Experiments", *IEEE/ASME Transactions on Mechatronics*, vol. 18, (5), pp.1527-1534, 2013.

[5] S. Anton and D. Inman, "Vibration Energy Harvesting For Unmanned Aerial Vehicles", *Active and Passive Smart Structures and Integrated Systems*, vol. 6928 (24), 2, 2008.

[6] A. Erturk and D. Inman, "On mechanical modeling of cantilevered piezoelectric vibration energy harvesters," *J. Intell. Mater. Syst. Struct.*, vol. 19, pp.1311-1325, 2008.
[7] GEMFAN, (2014), *Multirotor Propellers*, Website: available from, http://www.gemfanhobby.com/Product/Main/En/2a1a01aa-2fc5-42b6-a42c-a48800d8e5d8 (accessed on 10/01/2017).
[8] GrabCAD (a), (2014), *About GrabCAD*, Website: available from, http://resources.grabcad.com/company/ (accessed on 29/12/2016).
[9] GrabCAD (b), (2016) *GrabCAD*, Website: available from, https://grabcad.com/igor.lins.e.silva/about (accessed on 09/01/2017).